ENERGY ABSORPTION PROPERTIES OF CFRP COMPOSITES TUBE WITH DISCONTINUOUS PLIES

Zhibo Xin [1], Yugang Duan [2] and Jin Zhou [3]

[1] State Key Lab for Manufacturing Systems Engineering, Xi'an Jiaotong University, Xi'an, Shaanxi 710049, China
Email: zhiboxin@stu.xjtu.edu.cn
[2] tate Key Lab for Manufacturing Systems Engineering, Xi'an Jiaotong University, Xi'an, Shaanxi 710049, China
Email: ygduan@xjtu.edu.cn
[3] School of Engineering, University of Liverpool, Liverpool, L69 3GH, UK
Email: jinzhou@liv.ac.uk

Keywords: Energy absorption, Discontinuous plies, pseudo-ductility,Composite square tube

Abstract
The carbon fiber reinforced plastic (CFRP) composite with overlapped discontinuous plies have been proven to exhibit advanced pseudo-ductility. This paper aims to use a similar concept to design CFRP square tube and investigate the effect of energy absorption capability with two cut-ply strategy: i) the cut direction had an angle of α tilted respect the loading direction which is the axial direction of the square specimens; ii) the cut direction had an angle of β tilted follow the fiber orientation. The quasi-static axial compression tests are conducted to explore failure process, crashworthiness characteristics and the corresponding energy absorption mechanisms. Experimental results showed that cutting angle α and β have a significant influence on the energy absorption performance. Increasing the angle of α from 15° to 70° led to an increase in specific energy absorption (SEA) from 51.0J/g to 73.1J/g. On the contrary, SEA decreased (from76.7 J/g to 56.9 J/g) with increasing β. However, they all exceed the SEA of continuous specimen (56.2J/g). This work demonstrates that the energy absorption performance of composite tubes can be improved by proper selection of cutting strategy and cutting angle.

1. Introduction

Passenger vehicles crashworthiness, which includes the ability to absorb energy and occupant protection, has been identified as a key area of focus to improve survivability in the event of a crash. Thin-walled tubular structures have been widely used by the motorsport and automotive industries as crashworthiness applications, such as automotive crash box. In view of previous works, some researchers have reported the use of CFRP to design and investigate crashworthy structures, ranging from geometric feature to failure trigger mechanisms. Feraboli et al.[1] conducted a systematic experimental investigation to evaluate the crush behavior of square tube with rounded corners. The effects of different corner radii on Specific Energy Absorption (SEA) value in compressive setups were highlighted. Palanivelu[2] et al. studied the quasi-static crushing characteristics and the corresponding of energy absorption composite tubes with nine different shapes. They found that the special geometrical shapes, such as hourglass and conical circular, were of excellent energy absorption capacity than that of the standard and uniform profiles. Siromani et al.[3] explored and compared the energy absorption capability of circular tubes with different failure trigger mechanisms. Their experimental results demonstrated that combining a chamfered tube with an inward-folding crush-cap yielded the lowest initial peak load and the highest SEA. Hussein et al.[4] performed experimental

studies on CFRP tubes wrapped externally with aluminum sheets crushed by a platen with cutting blades. Results showed that the specimens that platen with cutting blades had a lower initial peak force and higher mean crushing force compared with those crushed by flat platens.

On the other hand, the effects of fiber orientation and thickness for all composite material systems, which include carbon/epoxy[5], glass/epoxy[6] and aramid/epoxy[7], and hybrid material systems[8] have been investigated. So far, all studies showed that the fiber reinforced composite (CFRP) have extensively proved to be a weight efficient energy absorber over the conventional metallic structures.

Previous research[9] has proved that the reasonable distribution of ply cuts can improve the energy absorption properties of circular tube with unidirectional fiber orientation follow the axial direction. Now, the study presented here aims at introducing the effect of energy absorption capability with two cut-ply strategy.

2. Experimental setup

2.1. Materials

The composite material system used in this study is the unidirectional T300/EM112 CFRP pre-preg carbon/epoxy tape (Hengshen CO., Ltd, China) of nominal cured ply thickness 0.135 mm and with a 12K tow. The mechanical properties of T300/EM112 laminate are presented in Table 1. The curing cycle provided by manufactures' guidelines, which consist of a 2 °C/min ramp to 80°C kept for 30min, and then a second heat ramp at 1.5°C/min is performed up to 130°C kept for 2h.

2.2. Specimens preparation

All tube specimens are carried out in a clean environment with a lay-up of $[\pm15]_7$. The entire manufacturing process of these bio-inspired CFRP square tubes can be divided in three steps as shown in Fig. 1. First, as shown in Fig.1 (A) and (B), the pre-preg tape is exactly cut at 10 mm intervals through a DCS-260 automated ultrasonic cutting machine (Gerber Technology CO., Ltd, USA). An enough uncut areas were reserved around the cutting areas in order to prevent the pre-preg tape scattered altogether. In order to investigate the influences of cut direction, two cut-ply strategy are fabricated: i) group 1: the cut direction had an angle of α tilted respect the loading direction which is the axial direction of the square specimens; ii) group 2: the cut direction had an angle of β tilted follow the fiber orientation. Second, Fig.1 (C) to (F), let two discontinuous pre-preg tapes is precisely lay-up together in the form of the ply cut interdigitated with location tool and vacuum sucker. Then the previous uncut areas are cut, the backing material removed and wrapped the discontinuous and interdigitated pre-preg tape around a mould of square steel pipe. Third, after curing and demoulding, the specimens are polished using 400 and 800 grade SiC to minimize edge effects and guarantee the plainness of the end face. A 45° tilted chamfer end of tube is fabricated to reduce the initial load peak[10]. After trimming, the length of the specimens is fixed to 69 mm with an inner side length of 25 mm and a wall thickness of 1.5 mm. The fabricated tube detailed information was tabulated in Table 1.

2.3. Test setup and testing procedure

Before compression testing, some preliminary fundamental parameters including length, diameter and weight were measured in order to calculate specific energy absorption (SEA) of each specimen. All the specimens manufactured are tested under quasi-static axial compression conditions to follow their crushing load-deformation evolution. An MTS (SANS) CMT5504 screw driven electromechanical test machine with a 50 kN load cell is used to carry out all tests. The specimens are compressed between two steel cross head at a displacement rate of 2mm/s.

According to the different cut-ply strategy, test specimens were divided into two groups. Group 1: these tubes had α of 15°, 30°, 45°, 70° tilted respect the axial direction, which are corresponded with CA15, CA30, CA45 and CA70, respectively. Group 2: these tubes had β of 45°, 70°, 90° tilted follow the fiber direction and are abbreviated with CF45, CF70 and CF90, respectively. Except these two groups, two continuous square tubes as typical specimens are tested firstly.
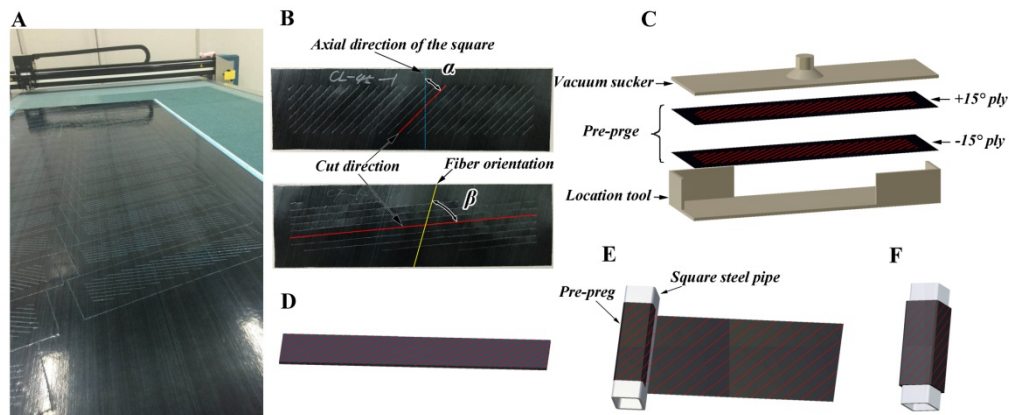
Figure 1. Manufacturing process of bio-inspired CFRP square tubes

Table 1. Geometric and crashworthiness characteristics of all specimens

Group number	Specimen number	Cut-ply strategy		M (g)	L (mm)	ΔL (mm)	F_{ip} (kN)	F_{max} (kN)	F_m (kN)	CFE (%)	EA (J)	SEA (J/g)
Group 1	C-1	-		20.2	69.1	50	24.7	24.7	16.2	65.6	810.6	55.5
	C-2			20.4	69.6		24.5	24.5	16.7	67.9	832.6	56.8
	Average			-	-		24.6	24.6	16.5	66.8	821.6	56.2
	CA15-1			20.4	70.0		23.9	23.9	15.2	63.4	758.6	52.1
	CA15-2		15	20.1	69.6		22.3	22.3	14.4	64.5	719.3	49.8
	Average			-	-		23.1	23.1	14.8	64.0	739.0	51.0
	CA30-1			20.2	69.4		25.1	26.2	18.5	73.7	925.9	63.6
	CA30-2	α=	30	20.7	70.5	50	23.0	26.0	18.9	82.1	944.8	64.4
	Average			-	-		24.1	26.1	18.7	77.9	935.4	64.0
	CA45-1			19.8	68.6		21.3	29.5	20.1	94.4	1005.5	69.7
	CA45-2		45	20.1	69.7		22.3	28.1	20.6	92.4	1028.2	71.3
	Average			-	-		21.8	28.8	20.4	93.4	1016.9	70.5
	CA70-1			19.9	69.5		22.9	28.2	20.9	91.2	1043.9	72.9
	CA70-2		70	19.7	68.9		23.9	27.9	20.9	87.4	1046.7	73.2
	Average			-	-		23.4	28.1	20.9	89.3	1045.3	73.1
Group 2	CF45-1			20.0	68.8		19.3	29.3	22.4	116.1	1122.2	77.2
	CF45-2		45	20.8	69.5		19.1	31.1	22.8	119.4	1140.0	76.2
	Average			-	-		19.2	30.2	22.6	117.8	1131.1	76.7
	CF70-1			20.3	70.1		19.7	26.5	19.4	98.5	971.6	67.1
	CF70-2	β=	70	20.2	69.6		19.4	25.1	19.6	101.0	977.8	67.4
	Average			-	-		19.6	25.8	19.5	99.8	974.7	67.3
	CF90-1			20.5	69.6		19.0	22.6	16.4	86.3	821.2	55.8
	CF90-2		90	20.1	69.3		20.3	23.7	16.8	82.8	840.4	57.9
	Average			-	-		19.7	23.2	16.6	84.6	830.6	56.9

3. Experimental results and discussion

3.1. Testing and observed failure of typical specimens (C)

The typical load-displacement cures and photographs of typical specimen before crushing and after crushing are shown in Fig. 2 and 3, respectively. As seen from Fig.2, the specimens C-1 and C-2 exhibit progressive failure process with good reproducible. The specimens start in a high initial peak force, Fmax, then the force drastically decline and finally it yield a low sustained crushing force, Fm. Their detailed information is tabulated in table 1.
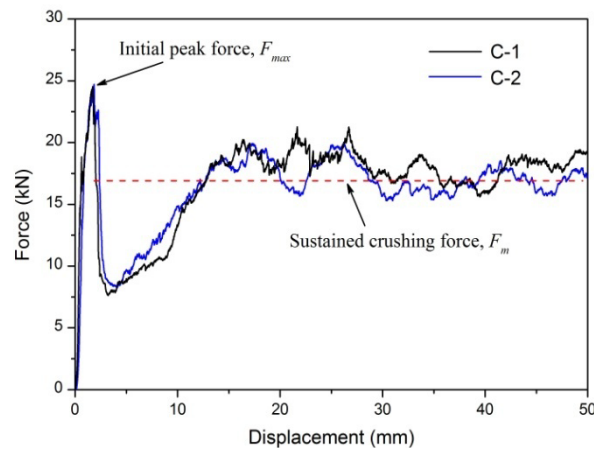
Figure 2. Typical load-displacement cures of continuous specimens C

The specimens C-1 and C-2 develop in the same deformation mode that the stable fracture started at the chamfered end of the specimen that is in contact with the upper support platen of the test machine. The crushing process begins with a catastrophic fracture in which the local wall and piles of tubes buckling. Whereafter, cracks appear due to the stress concentration on all four corners of the square tube, and propagated along the axial direction. The tube is eventually split into four sections by the cracks. This phenomenon is consistent with the frond fracture, which the tube wall is split into inner and outer fronds along the axial direction. Fig. 3 shows the specimen C-2 before crushing and after crushing.
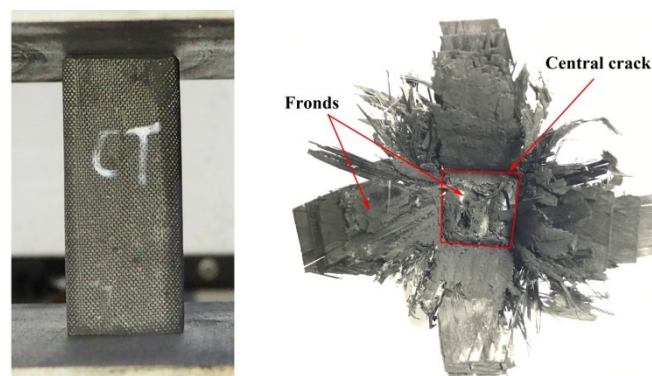

Figure 3. Photographs of typical specimen C-2 before crushing and after crushing

3.2. Testing and observed failure of group 1 specimens

Fig.4 shows the brief comparison of load-displacement curves for all types of group 1. It is noted that the curves of CA45 and CA70 located above the curves of CA15 and CA30. However, the load-displacement curve of CA70 exhibits more volatility during the firstly load drop.
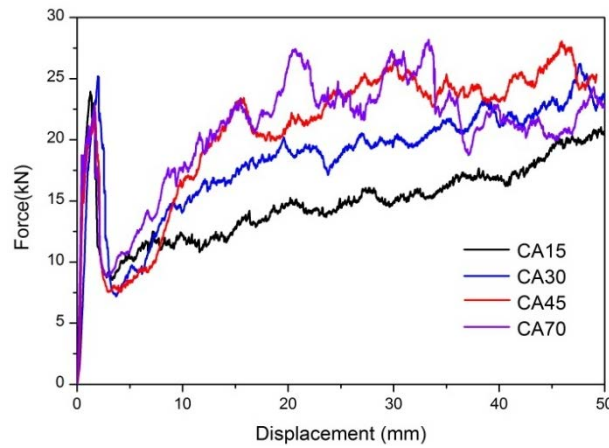

Figure 4. A comparison of load-displacement curves of four different cases in group 1

Due to the trigger mechanism, all specimens of group 1 with four different cutting directions tilted with respect to the loading direction are fracture at the chamfer end and exhibit excellently progressive failure progress. In sustained collapse stage, cracks appeared due to the stress concentration on all four corners of the square tube, in a manner similar to typical specimens. However, the tube walls are no longer yield to frond fracture but directly crush into debris especially CA70. Fig.5. shows the final deformation modes of all specimens of group 1. Clearly, it is found that the final mode of all specimens correspond to splaying progressive and transverse shearing mode, which is classified by Farley [11, 12]. The inner of all specimens in group 1 is filled with debris and inward fronds. From the comparison of the outward fronds of each case, it is interesting to note that for CA15 and CA30, their outward fronds are fairly complete and remained on the square tube wall, whereas for CA45 and CA70, more debris is formed. It means that the there are more crack produced in CA45 and CA70 in crushed process.
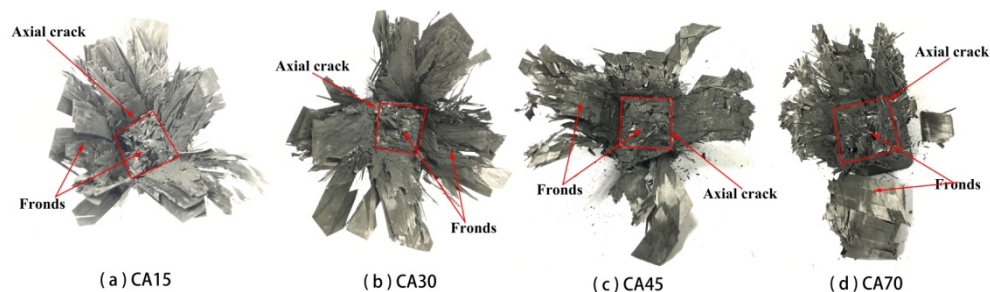

Figure 5. Final deformation of group 1 specimens

3.3. Testing and observed failure of group 2 specimens

Fig.6 depicts the comparison of load-displacement curves for all types of group 1. Clearly, it can be seen that the curves of CF45 located above the curves of CF70 and CF90.
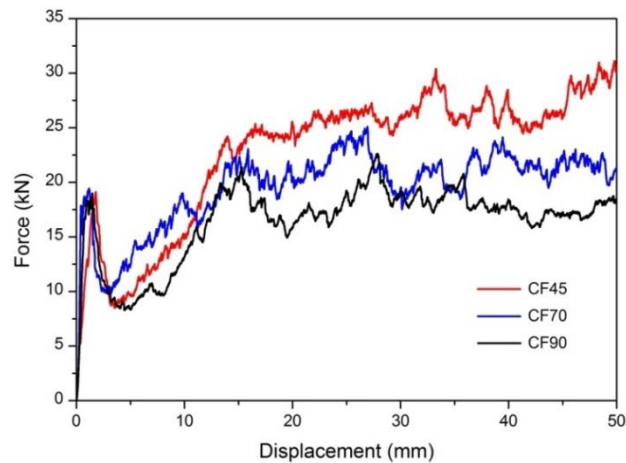
Figure 6. A comparison of load-displacement curves of four different cases in group 2

After initial cracks, the tube wall of all specimens of group 1 splits into inward and outward fronds, which is the same behavior as for typical specimens (C) and group 1 specimens (AC15, AC30, CA45 and AC 70). Fig.11 shows the final deformation mode of all specimens of group 2 under quasi-static axial compression. It is observed that the final mode of group 2 is similar to the group 1, which also belongs to splaying progressive and transverse shearing mode. Meanwhile it is interesting to find that for FC70 and FC90, their external and internal fronds break off mostly from the square tube wall, whereas for FC45, there is still some fronds remain. This means that the debris gradually became smaller and smaller with the increase of the ply-cut direction β. However, combining with the load-displacement curves of group 2, Fig.7, it can see that too small debris do not conducive the crush load increased.
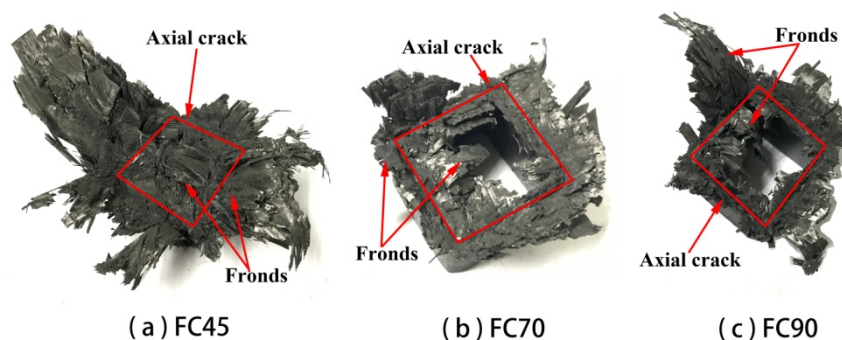

Figure 7. Final deformation of group 2 specimens

3.4. Specific energy absorption

Specific energy absorption is one of the most significant features to be used to value the crashworthiness and energy absorption capability in vehicles [13, 14]. Fig.8 (a) and (b) showed the effect of two types of cut-ply strategy with different α and β on SEA, respectively. The results exhibit a similar trend that has occurred in Energy absorption. As shown in Fig. 8 (a), it can be observed that increasing the angle of α from 15° to 70° led to an increase in SEA from 51.0J/g to 73.1J/g (as listed in table 1). Fig. 8 (b) plots the changed tend of SEA with different β in group2. In contrast of the two cut-ply strategy, the strategy for tilted follow the fiber direction exhibits more SEA value under quasi-

static axial compression conditions. The average SEA of FC45 (76.7J/g) slightly increase of 5% compare to the AC70 (73.1J/g).
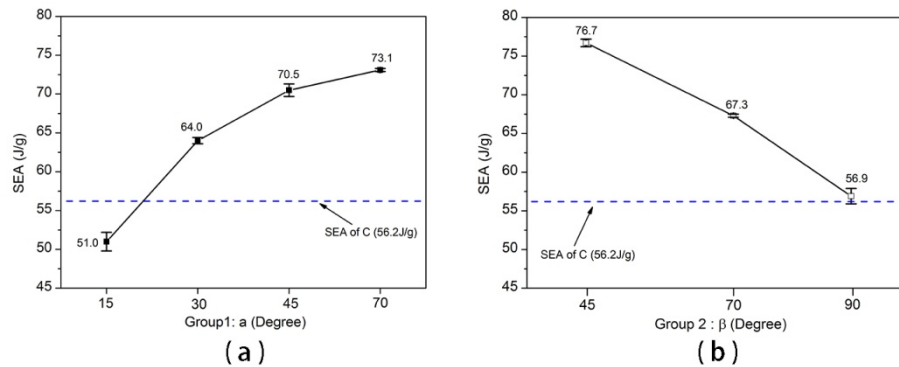

Figure 8. Graphical comparisons of (a) specific energy absorption for group 1, and (b) specific energy absorption for group 2

4. Conclusions

In this work, quasi-static axial crushing tests are performed to study the crashworthiness characteristics and the energy absorption mechanism of composite square tubes fabricated by two cut-ply strategies: i) the cut direction had an angle of α tilted respect the loading direction which is the axial direction of the square specimens; ii) the cut direction had an angle of β tilted follow the fiber orientation. Experimental results show that the effect of cutting angle α and β are proved to have a great influence on the energy absorption performance.

References

[1] Feraboli P, Wade B, Deleo F and Rassaian M. Crush energy absorption of composite channel section specimens. *Composites Part A: Applied Science and Manufacturing*. 2009; 40: 1248-1256.
[2] Palanivelu S, Van Paepegem W, Degrieck J, et al. Comparative study of the quasi-static energy absorption of small-scale composite tubes with different geometrical shapes for use in sacrificial cladding structures. *Polym Test*. 2010; 29: 381-396.
[3] Siromani D, Henderson G, Mikita D, et al. An experimental study on the effect of failure trigger mechanisms on the energy absorption capability of CFRP tubes under axial compression. *Composites Part A: Applied Science and Manufacturing*. 2014; 64: 25-35.
[4] Hussein RD, Dong R and Lu G. Cutting and crushing of square aluminium/CFRP tubes. *Compos Struct*. 2017.
[5] Bolukbasi A and Laananen D. Energy absorption in composite stiffeners. *Composites*. 1995; 26: 291-301.

[6] Mahdi E, Hamouda AMS and Sebaey TA. The effect of fiber orientation on the energy absorption capability of axially crushed composite tubes. *Materials & Design*. 2014; 56: 923-928.

[7] Farley GL. Effect of specimen geometry on the energy absorption capability of composite materials. *J Compos Mater*. 1986; 20: 390-400.

[8] Mahdi E, Hamouda AMS, Sahari BB and Khalid YA. Effect of hybridisation on crushing behaviour of carbon/glass fibre/epoxy circular–cylindrical shells. *J Mater Process Technol*. 2003; 132: 49-57.

[9] Xin Z, Zhang X, Duan Y and Xu W. Nacre-inspired design of CFRP composite for improved energy absorption properties. *Compos Struct*. 2018; 184: 102-109.

[10] Kim J-S, Yoon H-J and Shin K-B. A study on crushing behaviors of composite circular tubes with different reinforcing fibers. *International Journal of Impact Engineering*. 2011; 38: 198-207.

[11] Farley GL and Jones RM. Crushing Characteristics of Continuous Fiber-Reinforced Composite Tubes. *J Compos Mater*. 1992; 26: 37-50.

[12] Farley GL. *Relationship Between Mechanical-Property and Energy-Absorption Trends for Composite Tubes*. NASA Langley Technical Report Server, 1992.

[13] Xu F, Tian X and Li G. Experimental Study on Crashworthiness of Functionally Graded Thickness Thin-Walled Tubular Structures. *Experimental Mechanics*. 2015; 55: 1339-1352.

[14] Solaimurugan S and Velmurugan R. Progressive crushing of stitched glass/polyester composite cylindrical shells. *Composites Science & Technology*. 2007; 67: 422-437.